We are IntechOpen, the world's leading publisher of Open Access books Built by scientists, for scientists

4,800
Open access books available

122,000
International authors and editors

135M
Downloads

Our authors are among the

154
Countries delivered to

TOP 1%
most cited scientists

12.2%
Contributors from top 500 universities

CLARIVATE ANALYTICS BOOK CITATION INDEX INDEXED

WEB OF SCIENCE™

Selection of our books indexed in the Book Citation Index in Web of Science™ Core Collection (BKCI)

Interested in publishing with us?
Contact book.department@intechopen.com

Numbers displayed above are based on latest data collected.
For more information visit www.intechopen.com

30

A Novel Autonomous Climbing Robot for Cleaning an Elliptic Half-shell

Houxiang Zhang[1], Rong Liu[2], Guanghua Zong[2], Jianwei Zhang[1]
[1]*University of Hamburg*
Germany
[2]*Beihang University*
China

1. Introduction

At present a large number of high-rise buildings with curtain glass walls are emerging in modern cities. Cleaning the outer surface of these buildings is dangerous and laborious work in mid-air. Currently, most buildings are still cleaned manually with the help of a Gondola system or even a simple tool. The number of buildings with complicated shapes is increasing worldwide. Even skilled workers with safety ropes have difficulties in climbing those buildings. The development of walking and climbing robots offers a novel solution to the above-mentioned problems. Because of the current lack of uniform building structures, wall cleaning and maintenance of high-rise buildings is becoming one of the most appropriate fields for robotization (Zhang, H. et al., 2004).

In the last two decades, several different prototypes were designed for this purpose (Sattar, T. P., et al., 2003), (Briones, L. et al., 1994), (Luk, B. L. et al., 2001), (Liu, S. et al., 2000). The development and application of cleaning robotic systems can make the automatic cleaning of high-rise buildings possible and thus relieve workers of this hazardous task; furthermore it can improve the level of technology in building maintenance. Although several robots have already been developed for wall cleaning, most of them can only deal with uniformly shaped planes. We have been developing a family of autonomous Sky Cleaner climbing robots with sliding frames for glass-wall cleaning since 1996. The first model (Zhang, H. et al., 2004) has only limited dexterity and cannot work on a vertical wall. Because it lacks a waist joint, the robot is unable to correct the direction of its motion. As it takes the system a long time to deal with and cross obstacles, its cleaning efficiency is only 37.5 m^2/ hour. The second robot (Zhang, H. et al., 2004) is easily portable and has a cleaning efficiency of about 75 m^2/ hour. But the stiffness of the construction is very low, causing a small distortion during cleaning and climbing activities. Sky Cleaner3 is a commercial product which is driven by pneumatic cylinders and attaches to glass walls with vacuum suckers (Zhang, H. et al., 2005). However, this prototype cannot be used on any other type of walls.

SIRIUSc (Elkmann, N. et al., 2002) is a walking robot for the automatic cleaning of tall buildings and skyscrapers. This robot can be used on the majority of vertical and steeply inclined structured surfaces and facades. However, it cannot move sideways on its own and has to be positioned this way by a trolley on the top of the roof. Another robot was developed for the Leipzig Trade Fair in 1997 (Elkmann, N. et al., 2002). It was the first facade cleaning robot for vaulted buildings worldwide. Because of this vaulted construction of the surfaces to be cleaned, the robot is a very specialized system and not designed modularly.

Source: Mobile Robots Towards New Applications, ISBN 3-86611-314-5, Edited by Aleksandar Lazinica, pp. 784, ARS/plV, Germany, December 2006

In this chapter, based on analyzing the characteristics of the working target, a new kind of auto-climbing robot is proposed, which is used for cleaning the spherical surface of the National Grand Theatre in China. The robot's mechanism and its unique aspects are presented in detail. A distributed controller based on a CAN bus is designed to meet the requirements of controlling the robot. The control system is divided into six parts, five CAN bus control nodes and a remote controller, which are designed and established based mainly on the microprocessor P80C592.
Then the motion functions are described in detail. From the safety point of view, the process of climbing from one strip to another is very dangerous because the robot has to adapt to the outer shape of the building. Additionally, this robot has to be quite big in order to realize all necessary functions. Therefore, in designing this mechanism and its controls, an equilibrium between safety and size has to be reached. This is why the kinematics model of the climbing process is introduced. For system design and control purposes, the dynamics of the robot are calculated by applying the Lagrange equation. The force distribution of the front and rear supporting mechanisms is computed in a way that ensures the safety of the climbing process. After that, a new approach to path planning for wall-cleaning robots is presented considering movement security, cleaning efficiency and the percentage of cleaning coverage. The successful on-site test confirms the principles described above and the robot's ability to work on a spherical surface.

2. Overview of the robot system

2.1 Cleaning Target

An auto-climbing robot for cleaning glass walls with a complicated curved surface was developed in 2002 (Zhang, H., 2003). Taking the National Grand Theatre of China as the operation target, the robot can autonomously climb and clean its covering outer walls shaped in a half-ellipsoid. The theatre is 54 m high, and the long axis and short axis of the ellipse on the ground are 212 m and 146 m respectively, as shown in Figure 1. The surface walls consist of more than 20,000 glass and titanium planks. The total outer surface covers 36,000 m^2, with 6,000 m^2 of transparent glass walls, and 30,000 m^2 of Titanium walls (Liu, R. et al., 2003). The wall consists of 54 strips altogether, with each strip having a different height and sloping angle, as shown in Figure 2. The outer surface holds some LED-lamps, decorating belts and tracks. A track which was originally designed for the needs of construction and maintenance circles the half-ellipsoid along the rim between every two strips. In order to achieve a half-ellipsoid, each plank is constructed at a different size and is connected to its surrounding planks at an angle.

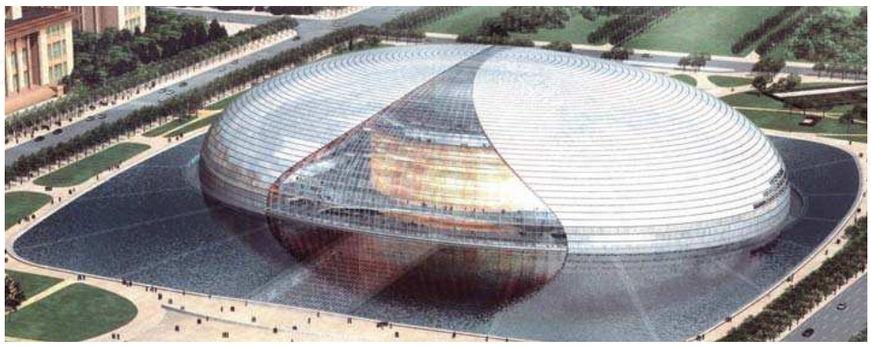

Fig. 1. National Grand Theatre of China.

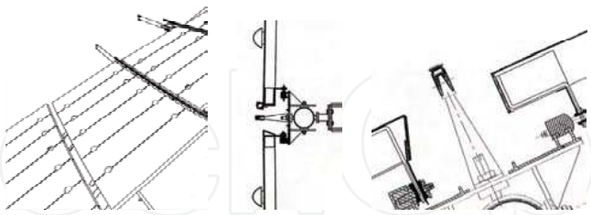

Fig. 2 Features of the working target.

2.2 Mechanical design

Based on the features of the construction mentioned above, an auto-climbing robot is designed as shown in Figure 3. The robot independently climbs and descends in the vertical direction and cleans in the horizontal direction. It takes the circling tracks as supports for climbing up and down between strips and moving horizontally along one strip around the ellipsoid. Its body consists of the climbing mechanism, the moving mechanism, two cleaning brushes and the supporting mechanisms. The robot is 3 meters long, 1.5 meters wide and 0.4 meter high. In order to keep the weight light while maintaining a dexterous movement mechanism, considerable stress is laid on a light yet stiff construction. Most of the mechanical parts are designed specifically for the robot and mainly manufactured in aluminium.

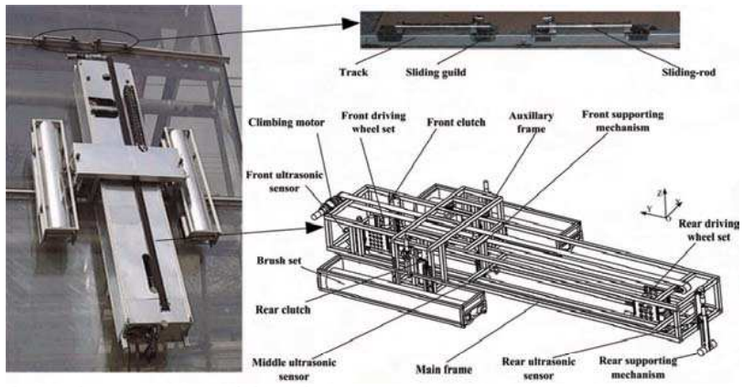

Fig. 3 Mechanical construction of the robot.

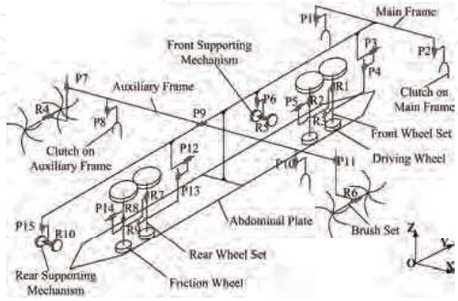

Fig. 4 Degree of freedom.

The degree of freedom of the robot is demonstrated in Figure 4. There are 25 joints altogether, 17 out of which are active and are actuated by respective DC motors. The joints are categorized and described as follows:

1 Linear active motion between the main frame and the auxiliary frame (P9);
2. Linear active motion of two rod-clutches on the main frame (P1, P2);
3. Linear active motion of two rod-clutches on the auxiliary frame (P8, P10);
4. Linear active motion of the front and rear supporting mechanisms (P6, P15), and passive rotation of wheels on the front and rear supporting mechanisms (R5, R10);
5. Three rotary joints (R1, R2, R3) and three prismatic joints (P3, P4, P5) on the front driving-wheel set.
   R1 represents the active rotation of the driving wheel;
   R2 is the passive rotation of the wheel paired to the driving wheel;
   R3 is a passive rotation which is used for the wheels to adapt the angle to the track;
   P3 is a linear passive motion used for the front wheel set to adapt its relative position to the track;
   P4 is the linear active motion to lift or lower the wheels;
   P5 is used to clamp the track between the wheels.
6. The joints on the rear wheel set are similar to those of the front wheel set.
7. Linear active motion of the left and right brush-sets (P7, P14), and active rotation for the left and the right brushes (R4, R5).

2.3 Mechanical realization

The main body of the robot is made up of two frames: the main frame and the auxiliary frame. Other functional parts are all mounted on these two frames. The auxiliary frame can slide along the main frame. This linear movement is actuated by the DC motor and the belt, both of which are mounted on the top of the main frame (shown in Figure 5).

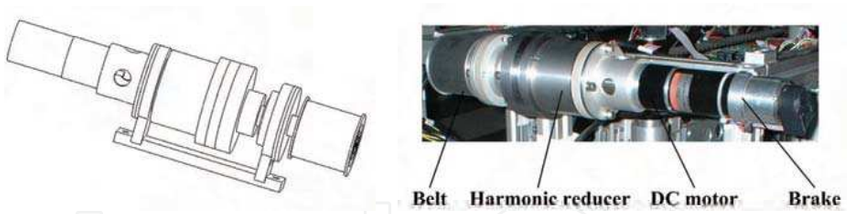

Fig. 5. The climbing mechanism.

The auxiliary frame has a shape like an "n" encircling the main frame to ensure safe and reliable movement (shown in Figure 6). A special sliding bar made of polyethylene is designed to create a sliding-mate between the two frames thus saving the weight of the linear guidance which is usually used for this kind of structure. Two rotating brushes mounted on the auxiliary frame move up and down and rotate for cleaning when the robot moves sideways along the tracks.

There are two pairs of clutches (shown in Figure 7) on the main frame and the auxiliary frame respectively. Their function is to grasp the sliding-rods which safely slide along the track without becoming detached. The sliding-rods are designed to be the medium between the track and the robot in order to avoid the safety problem caused by the robot directly grasping the track. A DC motor is embedded in the mechanical clutch which allows for a very slight structure. Three switches on the top, in the middle and at the bottom are used to feedback its vertical movement.

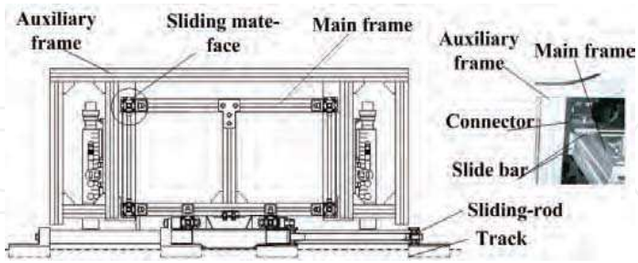

Fig. 6. Sliding-mate between two frames.

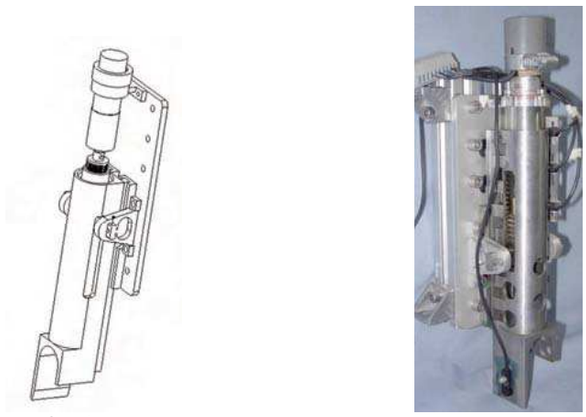

Fig. 7. The clutch mechanism.

A front supporting mechanism and a rear supporting mechanism with the same structure as the clutches are used to adjust the orientation of the robot and support the body on the surface. There are two supporting wheels on the tip of the mechanism in order to increase the area of interaction and avoid damaging the surface (shown in Figure 8). The wheels give a passive turning motion when the robot climbs in the vertical direction.

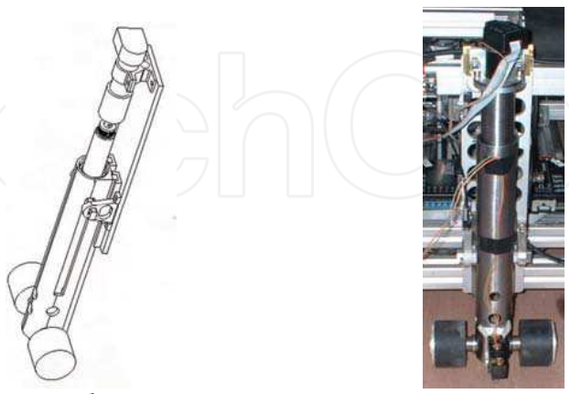

Fig. 8. The supporting mechanism.

A front and a rear wheel set which are used to provide the sideways driving force for the robot when they are clamped on the tracks are also installed on the axis of the main frame. The rear wheel set can move passively along the middle axis of the main frame in order to suit the various sizes of the planks caused by the arc shape of the building surface (as shown in Figure 9). A linear guidance connects the whole set to the main frame, which permits a passive sliding. The lifting DC motor can lift and lower the whole set to adapt to the height of the track.

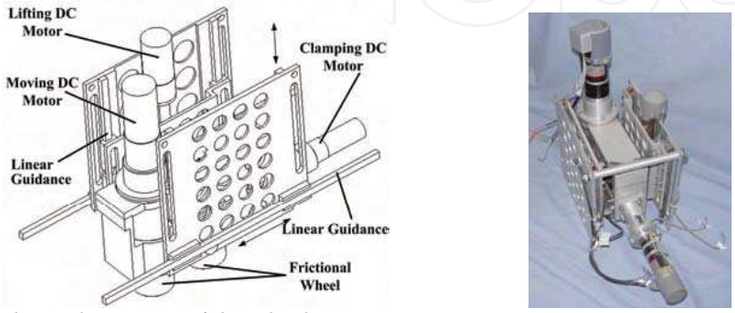

Fig. 9. Mechanical structure of the wheel set.

When the robot is working on such a half-ellipsoid, obstacles and the friction make it almost impossible to attach a safety cable to the robot from the theatre top. As a result, a special mechanical structure named the abdominal plate was developed and designed to solve the safety problem. While a set of clutches hold the sliding-rod to avoid falling down, the abdominal plate on the robot is interposed between two little wheels on the sliding-rod to avoid capsizing out of the wall (shown in Figure 10).

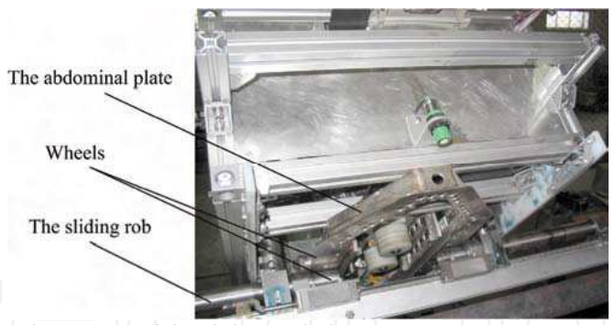

Fig. 10. Mechanical structure of the abdominal plate.

Table 1 summarizes the main specifications of the robot.

Body Mass (kg)	100
Body Mass (mm^3): Length ×Width ×Height	2800 ×1384×360
Cross obstacles (mm^2): Height ×Width	150×100
Max climbing velocity (mm/s)	50
Max working height (m)	50
Cleaning efficiency (m^2/ hour)	>100

Table. 1. Specifications of the robot.

3. Design of the distributed control system

3.1 Distributed Control System Based on CAN Bus

Five key issues are essential for this big and complicated robotic control system: a) functionality, b) safety c) extensibility, d) easy handling, e) and low cost. A distributed control system based on CAN bus is adopted to satisfy these issues, as shown in Figure 11. The system is divided into 6 parts, five CAN bus control nodes and a remote controller (Zhang, H. et al., 2005).

The PCM-9575 industrial PC (IPC) is the core part of the control system. It is a new EBX form factor 5.25" single board computer (SBC) with an onboard VIA Embedded low power Ezra 800 MHz. The VIA Eden processor uses advanced 0.13µ CMOS technology with 128KB L1 cache memory and 64KB L2 cache memory. This board can operate without a fan at temperatures up to 60° C and typically consumes fewer than 14 Watts while supporting numerous peripherals. This SBC includes a 4X AGP controller, a PCI audio interface, a PCI Ethernet interface, and 2 channel LVDS interfaces. Its design is based on the EBX form factor that supports the PC/104-Plus interface for ISA/PCI module upgrades. Other onboard features include a PCI slot, an LPT, 2 USBs, IrDA and 4 serial ports.

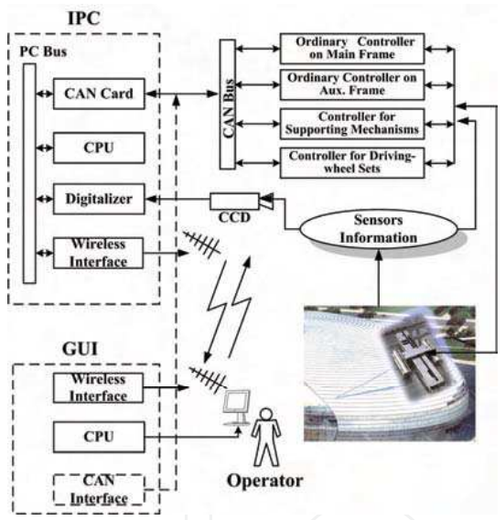

Fig. 11. Control system.

A PCM3680 card is used as a communication interface with PC/104-Plus interface for the main node and the other CAN nodes. The main computer node is a higher-level controller and does not take part in joint motion control. The responsibilities of the main computer node include receiving orders from the remote controller, planning operational processes, receiving feedback information from other nodes, and giving orders to other nodes. The other four lower-level nodes are responsible for receiving orders from the main computer node and directly controlling respective joint motors.

It is important for the control system to realize precise position control when the robot moves vertically from one strip of planks to another. On the other hand, some joints such as brushes and clutches only need an ordinary on-off control mode. As a result, two kinds of CAN nodes, both designed by us and mainly based on the P80C592 micro-chip, are included in the control system in

order to meet the requirements of functionality, extensibility and low cost. Each node is in charge of special functions in which all the related sensor signals are included.
For example, the supporting mechanism node can count the pulse signals from the encoder, deal with the signals from the touchable sensors and other magnetic sensors, and directly drive the DC motors in the front and rear supporting mechanisms. To make the control node extensible, it contains enough I/O resources which allow for the easy attachment of sensors and sensor processing equipments. At the same time multiple process programming capability is guaranteed by the principle of CAN bus.
Controlling and monitoring the robot is achieved through the digitalized CCD camera and a wireless graphical user interface (GUI) which allows for an effective and friendly operation of the robot. Once the global task commands are entered by the user, the robot will keep itself attached to and move on the surface while accomplishing its cleaning tasks. All information from its activities will be sent back to and displayed on the GUI during the phase of the feedback. In order to check out the rationality and safety of the task commands, they first have to be remembered. The following part includes command interpretation, task-level scheduling, and motion planning.

3.2 Sensor System

Multiple sensing and control systems are incorporated to handle uncertainties in the complex environment and realize intelligent climbing and cleaning motions. Software should be dexterous enough to identify the various geometries of the wall and intelligent enough to autonomously reconstruct the environment. The robot's body does not interact with the planks due to its particular mechanical structure. The tracks and the sliding-rods on the building surface are two important targets to be detected when the robot climbs and cleans.
All the sensors on the robot, which can be divided into external and internal sensors, are shown in Figure 12. The internal sensors reflect the self-status of the robot. There are 48 limit switches in total. For each active joint, magnetic limit switches give the controller the position of the joint. In order to increase the detection diameter, a magnetic metal slice is placed at a specific position. The test results show that the reliability of the sensor signal is guaranteed and the diameter for detection is 0-3mm. For the climbing movement mechanism and the supporting mechanisms where the accurate position is needed, the HEDL55 optical encoders from MAXON Company are used. The control node can directly count the pulse signals from the encoder using the interruption.

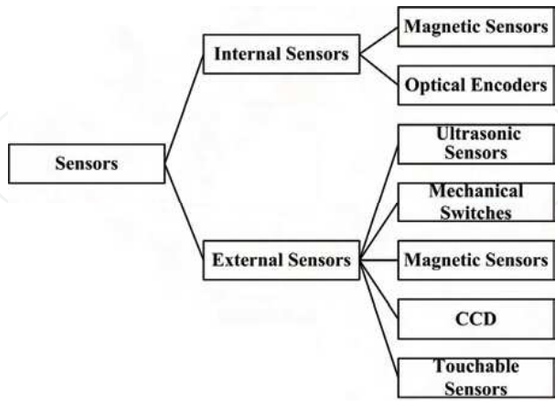

Fig. 12. Sensor system.

The external sensors are responsible for collecting information about the operational environment. All of them are very important for work safety. There are three ultrasonic analog sensors placed at the front, in the middle and in the rear parts respectively. First and foremost they detect the sliding-rod in the moving direction. The accuracy of the sensors' output is affected by three issues including the temperature, the distance for detection, and the reflection performance of the objects. The US25 from TAKEX Company is chosen for our control system. The distance for detection is 5-25 mm; the precision for distinguishing is 40 mV/mm; the velocity for responding is 50 ms and the operating temperature is –10 - 55 degrees Celsius. The output of the ultrasonic analog sensor when detecting sliding-rods on the plank is shown in Figure 13.

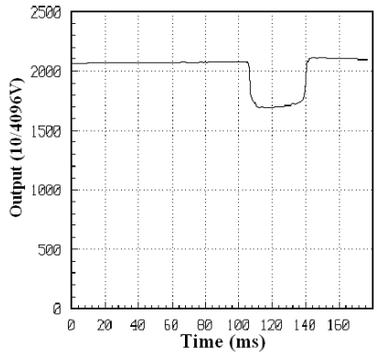

Fig. 13. Experiment result of the ultrasonic sensor.

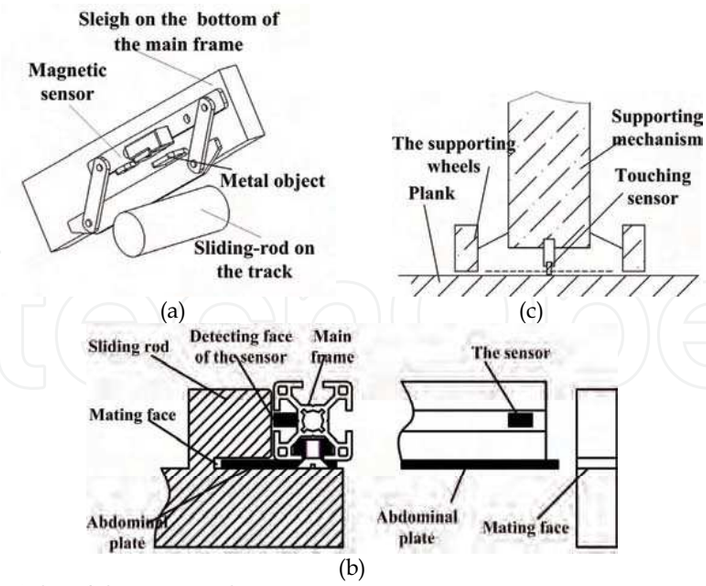

Fig. 14. Principles of three external sensors.

There is an outshoot if the sensor detects something above the plank. On the other hand, any two signals can be used to compute the angle between the robot frame and the plank. To obtain precise data, the software will firstly choose the data and get rid of the mistakes, and then use the middle filter and the average filter for correcting the data, yielding accurate data for computing.

After the position of the sliding-rod is established during the climbing movement, the robot main frame will pitch down and make contact with the sliding-rod controlled by the supporting mechanisms. We designed a kind of mechanical touchable sensor for detecting the interaction between the main frame and the sliding-rods. Figure 14(a) depicts its structure, for which a mechanical parallelogram was used. When the bottom of the main frame touches the sliding-rod, the contact force deforms the parallelogram, whereon the magnetic sensor sends a signal to the controller as soon as it has detected the metal object inserted for detection purpose.

Meanwhile, the magnetic sensors are used for monitoring how safe the connection between the abdominal plate and the sliding-rod is (shown in Figure 14(b)). When the robot is working, there should be at least one magnetic sensor available for detecting the abdominal plate inserted between two little wheels on the sliding-rod.

There are two touchable sensors on the tip of the front and the rear supporting mechanisms, which are used to monitor the interaction condition of these supporting mechanisms and to determine whether the attachment to the surface is stable (shown in Figure 14(c)).

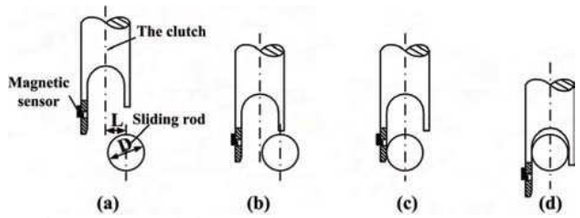

Fig. 15. The process of grasping a sliding-rod.

Some magnetic sensors are mounted on the clutches to ensure reliability when the clutches set out to grasp the sliding-rod. The process of grasping is shown in Figure 15.

(a) The clutch is positioned over the sliding-rod in order to satisfy the following formula: $L>D/2$;
(b) The clutch lowers until the middle switch on the clutch mechanism gives a signal;
(c) The movement of the clutch towards the sliding-rod will stop when the magnetic sensor set off;
(d) The clutch is lowered until the process is finished.

4. Movement realization

Movement realization includes two parts: climbing movement and cleaning movement. The robot can climb in the vertical direction and clean in the horizontal direction.

4.1 Climbing movement

Figure 16 shows the process of climbing from one layer to the next. In this process the brush sets are all in the up-state (no contact with the plank).

(a) The robot is in its home state: clutches on the main and auxiliary frame are all in the down-state to hold the sliding-rod on track 1 and on track 2 respectively; the

abdominal plate is inserted in both sliding-rods; the two supporting mechanisms are all in the up-state.

(b) Clutches on the auxiliary frame are raised, and the auxiliary frame is pulled up along the main frame.

(c) The motion of the auxiliary frame stops when the clutches on it are right above track 2. Then the clutches are lowered to grip the sliding-rod.

(d) Clutches on the main frame are raised; the front supporting mechanism touches down on plank 1.

(e) The main frame moves up. When the abdominal plate is out of the sliding-rod on track 1 and the rear supporting mechanism is above plank 1, the main frame stops moving and the rear supporting mechanism touches down on plank 1.

(f) The front supporting mechanism is raised, and the main frame continues to move up. When the front supporting mechanism is above plank 2, it touches down on plank 2.

(g) The upward movement of the main frame does not stop until track 3 is detected by the front ultrasonic sensor. Then the front or rear supporting mechanisms are adjusting to position the robot parallel to plank 2. Afterwards, the main frame moves up to insert the abdominal plate into the sliding-rod on track 3.

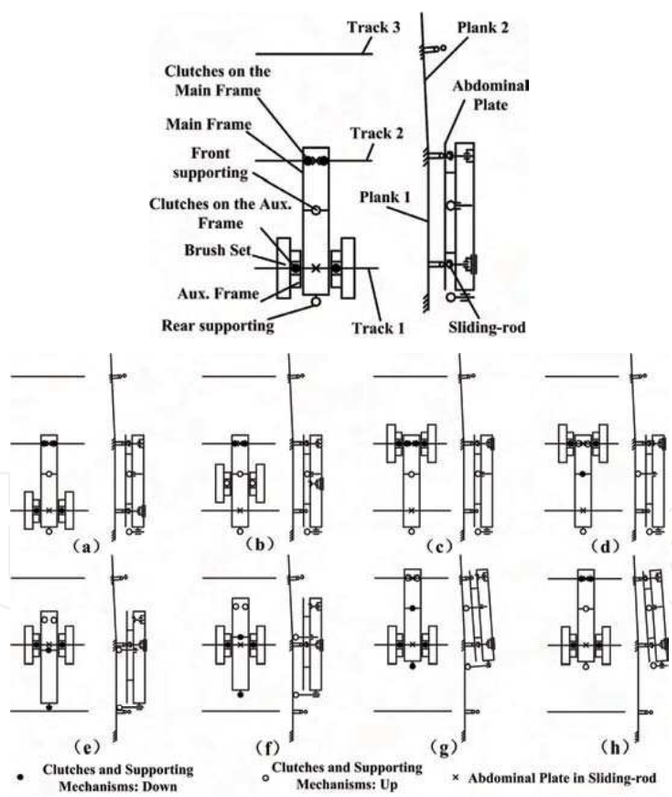

Fig. 16. Plan of the climbing motion.

(h) The motion of the main frame stops when the clutches on it are right above track 3. Then the clutches are lowered to grip the sliding-rod on track 3. The robot is now in its home state again, and the process of climbing up to the next strip is over.

4.2 Cleaning movement

Figure 17 demonstrates the process of the cleaning movement within one strip.

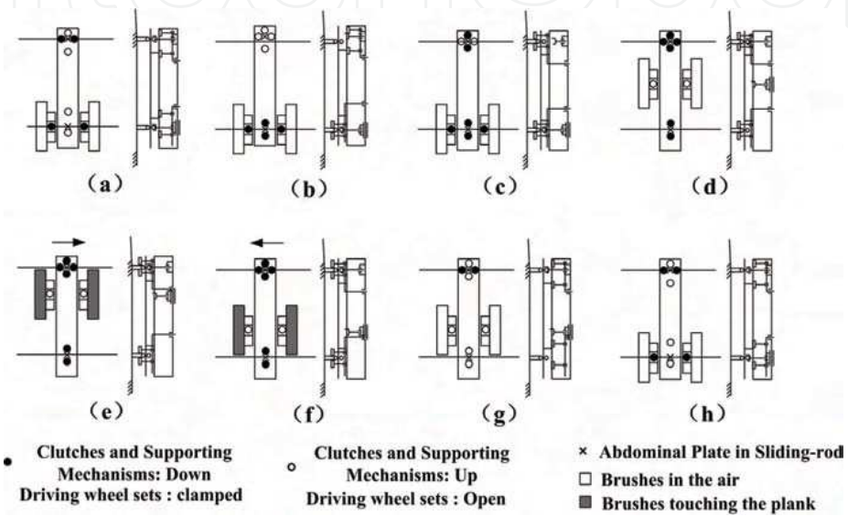

Fig. 17. Cleaning movement.

(a) The robot is in its home state.
(b) The clutches on the main frame are lifted. The main frame moves up until track 1 is right under the rear driving-wheel set. Then the rear wheel set is lowered and the driving wheels are clamped onto track 1.
(c) The main frame then moves down until track 2 is right under the front wheel set. Then the front wheel set is lowered and its driving wheels are clamped onto track2.
(d) Because the clutches on the main frame are in line with the front wheel set, the clutches can be put down to hold the sliding-rod on track 2. Then lift the clutches on the auxiliary frame.
(e) The auxiliary frame moves up until the upper edge of the brush-set is in line with track 2. Then the brush-set is lowered till it touches the plank. After the front and rear driving wheels are actuated simultaneously the robot can move to the right to clean the upper half of that strip.
(f) After a circle of one half-strip has been cleaned, the brush-set moves down to the lower half of that strip, and the robot moves left to clean that half.
(g) When the cleaning of that strip is finished, the brush-sets are lifted. Then both driving-wheel sets unclamp from the tracks and are lifted.
(h) After that, the clutches on the auxiliary frame move down with the frame to track 1, and are lowered to grasp the sliding-rod on track 1. Now the robot is back in its home state again.

5. Climbing dynamics

5.1 Kinematics analysis

The robot autonomously climbs and cleans the elliptic surface. From the safety point of view, the process of climbing from one strip to another is very dangerous because the robot has to adapt to the shape of the building. Additionally, this robot has to be quite large in order to realize all necessary functions. Therefore, in designing the mechanism of this system and its controls, an equilibrium between safety and size has to be reached. In this section, the climbing dynamics of the robot are calculated based on the Lagrange formulation. We only discuss the process of ascending because the process of descending is similar.

There are two phases during the process of ascending. First the auxiliary frame moves along the main frame, then the main frame ascends. The first part is very safe due to the clutches holding the sliding-rod and the abdominal plate inserted into two sets of sliding-rods. We will only discuss the second part in detail.

The climbing dynamics of the robot are analyzed by the application of the Lagrange equation, described as (1) (Fu, K.S. et al., 1987).

$$\frac{d}{dt}\left(\frac{\partial L}{\partial \dot{q}_j}\right) - \frac{\partial L}{\partial q} = F_j, j = 1,2,3 \tag{1}$$

Where F_j is the generalized forces; L is the Lagrange function, as shown in (2).

$$L = T - V \tag{2}$$

Where T is the kinetic energy of the system; and V is the potential energy. We can change (1) into the following format (3).

$$M(q)\ddot{q} + C(q,\dot{q})\dot{q} + N(q,\dot{q}) = F \tag{3}$$

Where F is the generalized driving force; q is the generalized coordinate; $C(q,\dot{q})\dot{q}$ described with (4) is decided by the factors of the Coriolis force and the centrifugal force; $N(q,\dot{q})$ is decided by the nonconservative and conservative forces. Furthermore it can be described as (5) when the friction is neglected.

$$C_{ij}(q,\dot{q}) = \frac{1}{2}\sum_{k=1}^{n}\left\{\frac{\partial M_{ij}}{\partial q_k} + \frac{\partial M_{ik}}{\partial q_j} - \frac{\partial M_{kj}}{\partial q_i}\right\}\dot{q}_k \tag{4}$$

$$N_i(q,\dot{q}) = \frac{\partial V}{\partial q_i} \tag{5}$$

The kinematics model of the robot during climbing is shown in Figure 18. Where oxyz is the world coordinate and the xoy plane is paralleled with the lower plank; and o′x′y′z′ is the reference coordinate fixed at the robot's body, with the x′ axis along the width of the frame, the y′ axis along the length and the z′ axis pointing vertically upward from the main frame. The two points of o and o′ are superimposed.

In Figure 18 below, the parameters are shown (Zhang, H. et al., 2005).

r_3 is the vector from the centroid of the auxiliary frame to the centroid of the mainframe;

r_4 is the displacement of the front supporting mechanism;

r_5 is the displacement of the rear supporting mechanism;

β is the rotating angle of the mainframe according to the x axis, it is also named θ_x;

φ is the rotating angle of the mainframe according to the z′ axis;
α is the angle between the lower plank and the gravity vector;
R is the length of the clutches;
L_1 is the distance between the front supporting mechanism and the centroid of the mainframe;
L_2 is the distance between the rear supporting mechanism and the centroid of the mainframe;
m_1 is the mass of the mainframe;
m_2 is the mass of the auxiliary frame;
J_{1cx}, J_{1cy} and J_{1cz} are the moments of inertia of the mainframe;
J_{2cx} , J_{2cy} and J_{2cz} are the moments of inertia of the auxiliary frame;
F_{r3} is the driving force for climbing;
F_{FB} is the driving force for the front supporting mechanism;
F_{BB} is the driving force for the rear supporting mechanism;
M is the driving moment generated by the supporting mechanisms.

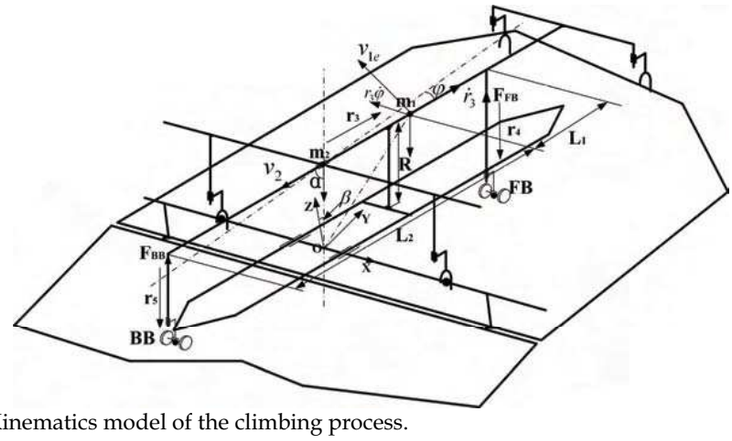

Fig. 18. Kinematics model of the climbing process.

When the front supporting mechanism is working, it is described as (6); when not, it is described as (7).

$$M = F_{FB} \times (L_1 + r_3) \tag{6}$$

$$M = F_{BB} \times (L_2 - r_3) \tag{7}$$

While climbing up, the front and rear wheel sets do not work so that the freedom in the x direction is not available. The freedom of climbing is three and can be described with the generalized coordinate q (r_3, φ, β). There are two situations that should be avoided during this process. One is the non-brace that means neither the front supporting mechanism nor the rear one works; the other is the excessive-brace that means two supporting mechanisms work together. There are some constraints between r_4, r_5 and β , as shown in (8) and (9).

$$\dot{r}_4 = (r_3 + L_1)\dot{\beta} \tag{8}$$

$$\dot{r}_5 = -(L_2 - r_3)\dot{\beta} \tag{9}$$

According to (2), the kinetic energy of the mainframe is T_1, as shown in (10).

$$T_1 = \frac{1}{2}m_1 v_{1c}{}^2 + \frac{1}{2}J_{1cz}\dot{\varphi}^2 + \frac{1}{2}J_{1cx}\dot{\beta}^2 \tag{10}$$

The absolute velocity of the mainframe v_{1c} is described as (11). The following velocity v_{1e} and the relative velocity v_{1r} are shown in (12), (13).

$$v_{1c} = v_{1e} + v_{1r} \tag{11}$$

$$v_{1e} = \sqrt{R^2 + r_3{}^2}\,\dot{\beta} \tag{12}$$

$$v_{1r} = \dot{r}_3 + r_3\dot{\varphi} \tag{13}$$

As shown in Figure 19, the vector $\dot{r}_3$ is orthogonal with $r_3\dot{\varphi}$, if v_{1e} and v_{1r} are projected along x′y′z′ coordinate axes; we can get (14).

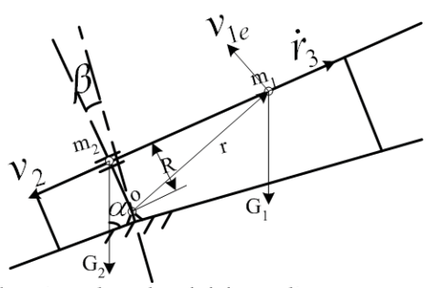

Fig. 19. Kinematics model projected on the x′y′z′ coordinate axes.

$$\begin{cases} v_{1c} = \sqrt{v_{1x'}{}^2 + v_{1y'}{}^2 + v_{1z'}{}^2} \\ v_{1x'} = r_3\dot{\varphi} \\ v_{1y'} = \dot{r}_3 - \sqrt{R^2 + r_3{}^2}\,\dot{\beta}\cdot\dfrac{R}{\sqrt{R^2 + r_3{}^2}} = \dot{r}_3 - R\dot{\beta} \\ v_{1z'} = \sqrt{R^2 + r_3{}^2}\,\dot{\beta}\cdot\dfrac{r_3}{\sqrt{R^2 + r_3{}^2}} = r_3\dot{\beta} \end{cases} \tag{14}$$

The kinetic energy of the mainframe is shown in (15).

$$T_1 = \frac{1}{2}m_1[(\dot{r}_3 - R\dot{\beta})^2 + (r_3\dot{\varphi})^2 + (r_3\dot{\beta})^2] + \frac{1}{2}J_{1cz}\dot{\varphi}^2 + \frac{1}{2}J_{1cx}\dot{\beta}^2 \tag{15}$$

Since the zero potential energy position is on the horizontal plane passing though point o, the potential energy is described as (16).

$$V_1 = m_1 gR\sin(\alpha - \beta) + m_1 gr_3\cos(\alpha - \beta) \tag{16}$$

In the same way, the kinetic energy and the potential energy of the auxiliary frame are calculated in the following (17), (18).

$$T_2 = \frac{1}{2} m_2 (R\dot{\beta})^2 + \frac{1}{2} J_{2cx} \dot{\beta}^2 \tag{17}$$

$$V_2 = m_2 g R \sin(\alpha - \beta) \tag{18}$$

In (19), all these results are inserted into the Lagrange function.

$$\begin{aligned} L = {} & \frac{1}{2} m_1 \dot{r}_3^2 + \frac{1}{2} m_1 R^2 \dot{\beta}^2 - m_1 R \dot{r}_3 \dot{\beta} + \frac{1}{2} m_1 r_3^2 \dot{\varphi}^2 + \frac{1}{2} m_1 r_3^2 \dot{\beta}^2 + \frac{1}{2} m_2 R^2 \dot{\beta}^2 \\ & + \frac{1}{2} J_{1cz} \dot{\varphi}^2 + \frac{1}{2} J_{1cx} \dot{\beta}^2 + \frac{1}{2} J_{2cx} \dot{\beta}^2 \\ & - m_1 g R \sin(\alpha - \beta) - m_1 g r_3 \cos(\alpha - \beta) - m_2 g R \sin(\alpha - \beta) \end{aligned} \tag{19}$$

According to the Lagrange equation (20), the dynamic characteristics of the climbing movement are reached, as shown in (21)-(23).

$$\begin{cases} \dfrac{d}{dt}\left(\dfrac{\partial L}{\partial \dot{r}_3}\right) - \dfrac{\partial L}{\partial r_3} = F_{r3} \\ \dfrac{d}{dt}\left(\dfrac{\partial L}{\partial \dot{\varphi}}\right) - \dfrac{\partial L}{\partial \varphi} = 0 \\ \dfrac{d}{dt}\left(\dfrac{\partial L}{\partial \dot{\beta}}\right) - \dfrac{\partial L}{\partial \beta} = M \end{cases} \tag{20}$$

$$m_1 \ddot{r}_3 - m_1 R \ddot{\beta} - m_1 r_3 \dot{\varphi}^2 - m_1 r_3 \dot{\beta}^2 + m_1 g \cos(\alpha - \beta) = F_{r3} \tag{21}$$

$$(m_1 r_3^2 + J_{1cz}) \ddot{\varphi} + 2 m_1 r_3 \dot{r}_3 \dot{\varphi} = 0 \tag{22}$$

$$\begin{aligned} & -m_1 R \ddot{r}_3 + (m_1 R^2 + m_2 R^2 + m_1 r_3^2 + J_{1cx} + J_{2cx}) \ddot{\beta} + 2 m_1 r_3 \dot{r}_3 \dot{\beta} \\ & -m_1 g R \cos(\alpha - \beta) + m_1 g r_3 \sin(\alpha - \beta) - m_2 g R \cos(\alpha - \beta) = M \end{aligned} \tag{23}$$

We can change the dynamic characteristics into format (3), as shown in (24). All of the results are important for system design and the design of the controlling mechanism.

$$\begin{aligned} M(q,\dot{q}) &= \begin{bmatrix} m_1 & 0 & -m_1 R \\ 0 & m_1 r_3^2 + J_{1cz} & 0 \\ -m_1 R & 0 & m_1 R^2 + m_2 R^2 + m_1 r_3^2 + J_{1cx} + J_{2cx} \end{bmatrix} \\ C(q,\dot{q}) &= \begin{bmatrix} 0 & -m_1 r_3 \dot{\varphi} & -m_1 r_3 \dot{\beta} \\ m_1 r_3 \dot{\varphi} & m_1 r_3 \dot{r}_3 & 0 \\ m_1 r_3 \dot{\beta} & 0 & m_1 r_3 \dot{r}_3 \end{bmatrix} \qquad F = \begin{bmatrix} F_{r3} \\ 0 \\ M \end{bmatrix} \\ N(q,\dot{q}) &= \begin{bmatrix} m_1 g \cos(\alpha - \beta) \\ 0 \\ -m_1 g R \cos(\alpha - \beta) + m_1 g r_3 \sin(\alpha - \beta) - m_2 g R \cos(\alpha - \beta) \end{bmatrix} \end{aligned} \tag{24}$$

5.2 The pitching forces

There are two kinds of dangerous cases during the climbing process, one is falling down and the other is capsizing out of the wall, as shown in Figure 20. The climbing robot has to be safely attached to the wall surface and has to overcome its gravity. The attachment plane should adapt to the complicated shape of the building. That is the first difference between a

wall climbing robot and an ordinary robot walking on the ground.
As mentioned before, the supporting mechanisms are used to adjust the alignment of the robot and to support the body on the surface. In order to meet the requirements of safety, the touching pressure between the supporting mechanisms and the surface should be sufficient. That means the interaction conditions on the surface are stable. On the other hand it is also quite dangerous if the force is too great as this could crush the planks. As N_{limit} (1500N) is the bearing capability of the plank, at the beginning of the designing process, we should make sure the touching pressure is smaller than this limitation.

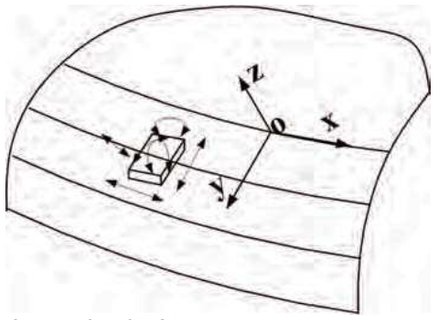

Fig. 20. Dangerous cases during the climbing process.

The front supporting force is shown in (25). Where L is the length of the mainframe; l is the negative of r_3 in order to compute the distribution of the force.

$$F_{FB} = \frac{G_2 \cdot R\cos\alpha + G_1 \cdot (R\cos\alpha + l\sin\alpha)}{-(L_1 - l)} \tag{25}$$

When all the conditions shown below apply, R = 150mm, L = 2800mm, G_1 = 60kg, G_2 = 40kg, L_1 = 200mm, L_2 = L/2=1400mm, a = 0-90°, the force distribution is gotten, as shown in Figure 21(a). Here the range of l should be within $[-1000,700]$ mm due to mechanical constrains. According to the same process, the distribution of the rear force is shown in Figure 21(b). From these two Figures, we can see the maximum of the supporting forces meet the requests, as shown in (26).

$$F_{BBmax} = 37.5Kg < F_{FBmax} = 88.6Kg < \boldsymbol{N_{limit}} \tag{26}$$

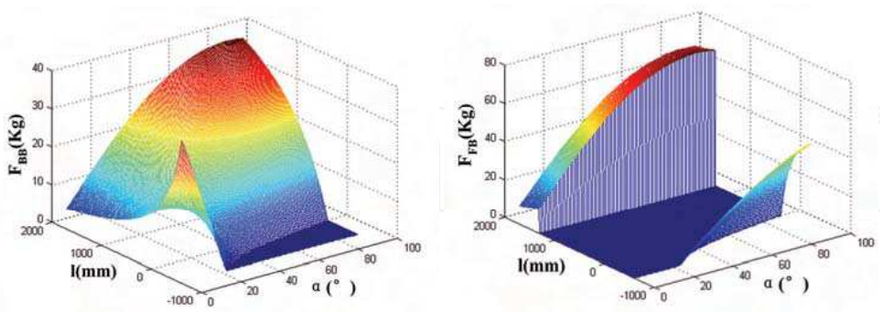

(a) (b)

Fig. 21. The front and rear supporting pressure distributions.

6. Cleaning Trajectory

6.1 Characteristics of path planning for wall cleaning robots

Another important issue for a wall-cleaning robot is path planning. A specific cleaning trajectory is essential for the cleaning movement to cover all the unoccupied areas in the environment. A lot of research has been devoted to the path planning problem, such as the grid-based method (Zelinsky, A., et al., 1993), the template-based method (Neumann de Carvalho, R. et al., 1997) and the neural network approach (Yang, S.H. et al., 2004). But none of these path planning methods can be directly used for the wall cleaning robot due to the characteristics of its special working environment.

Area-covering operation is a common and useful kind of path planning also named complete coverage path planning (CCPP), which requires the robot path to cover every part of the workspace (Hofner, C., et al., 1995) (Pirzadeh, A., et al., 1990). The CCPP is suitable for wall-cleaning robots due to robotic operational characteristics. This project is intended to develop an effective and easy-to-compute path planning for robotic cleaning systems on high-rise buildings. Even if the path planning methods for mobile ground-robots and those of wall-cleaning robots have a lot in common, the latter still feature three particular characteristics (Zhang, H., et al., 2005):

1) Prior knowledge of the global environment and local unexpected obstacles; the global environment is known in advance so that it can be considered as a static model. On the other hand, the work space includes numerous unexpected obstacles such as window frames and bars. From this point of view, the local work environment is dynamic and unknown. The cleaning trajectory is also based on local sensorial information.

2) Work environment constraints and cleaning function constraints; the robot should move in both the vertical direction as well as the horizontal direction to get to every point on the cleaning surface. In order to effect the cleaning, the robot has to face all obstacles and cross them safely and quickly so that the cleaning movement covers the whole area. At the same time, the climbing robot has to be safely attached to the glass wall and has to overcome gravity. The cleaning trajectory has to take both aspects into account.

3) Evaluation by synthesis of standards (Zhang, H., et al., 2005); the standards of choice and evaluation for the different kinds of path planning should synthesize work safety, cleaning efficiency and the percentage of cleaning coverage. The safety is the first important factor for

evaluation. But even if it is very reliable, the cleaning robot is still not a satisfactory product if it takes longer to clean a certain area than human workers would. The robot should find an efficient cleaning trajectory to carry out its work. At the same time, the percentage of cleaning coverage is also quite important from the practical point of view. It would be unacceptable for the robotic system to only achieve the cleaning of selected parts of the target surface while human workers in a gondola can clean it almost 100%.

6.2 Subdividing the work target

Path planning and the path tracking strategies for mobile robots are highly dependent on the work target characteristics. This project works with the concept of the limitation of the work area, so that the constructional consistency, continuity and accessibility are satisfied within any subdivided area. Consistency means the curtain-wall has the same structure within one area; continuity means that the area is a plane or a curve with a sufficiently large radius; and accessibility means that any spot on the wall can be reached. There are three guidelines for subdivision.

1) Boundary rule; on any work space there must be real horizontal and vertical boundaries which are natural marks for subdivision.
2) Medium rule; the work target can be subdivided into different parts according to its material. Generally, different methods and techniques for cleaning will be used on different planks.
3) Obstacle rule; there are many kinds of obstacles on the work space. The obstacles can be divided into four kinds: unexpected and expected obstacles according to their positions; dangerous and safe obstacles according to their criticality to the robotic system. Some obstacles are too high or too big for the robot to cross. They should be considered as a special, dangerous kind of boundary to be avoided.

Using these three guidelines, the global workspace can be subdivided into several regions, as shown in Figure 22. We are dealing with six work space regions. The material of Region I and IV is glass; other areas are Titanium.

Cleaning and walking are tracked by synchronizing the global information and the local perceived situation in the phase of path planning. Firstly the robot should choose a direction along which the cleaning work can be carried out. Here a representative subdivided area on the border between Region I and Region II, as shown in Figure 23, is the work target based on the principles of area definition.

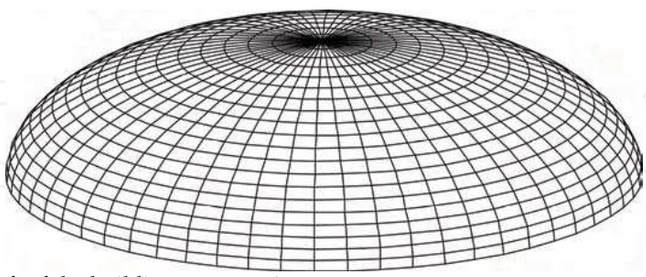

(a) The draft of the building construction.

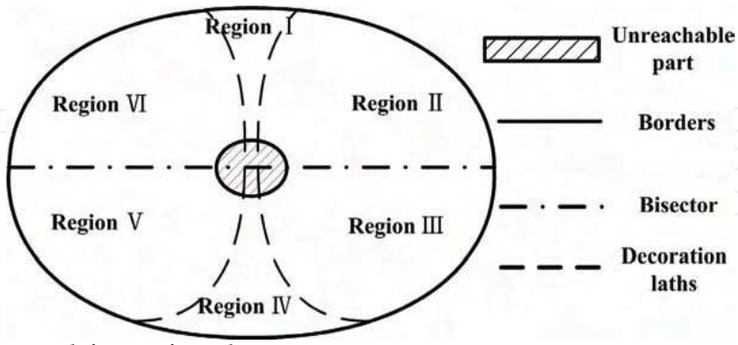

(b) Regions definition from the top view.

Fig. 22. Results of subdivision.

If the robot cleans the work space in the vertical direction, it has to cross the obstacles several times. It is much more difficult to clean the work target due to numerous horizontal obstacles. But the robot can clean uninhibited in the horizontal direction, because that way the wall is considered as forming a plane. The robot begins to clean the wall from the upper left point. It will move on to the next strip when the first strip of planks is finished cleaning. Some areas near the border cannot be cleaned for safety reasons. The coverage percentage on this small work area is over 95%. This value will be higher from the global point of view.

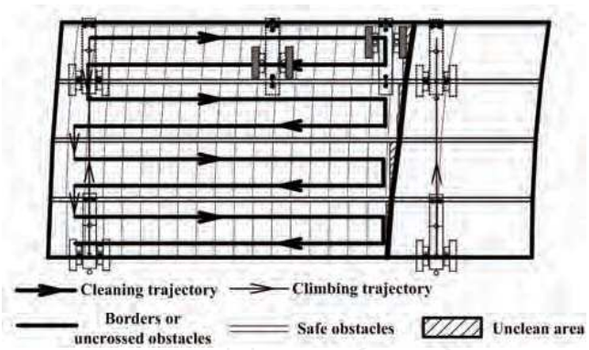

Fig. 23. Cleaning trajectory.

7. Conclusion

In contrast to conventional theoretical research, this project finishes the following innovative work:

1. This paper described a new kind of auto-climbing robot used for cleaning the complex curved surface of the National Grand Theatre in China. A special movement mechanism was developed and designed to satisfy weight and dexterity requirements. The robot has been tested on a demo wall which was built based on real building design. Figure 24 shows the robot climbing up in the same process as Figure 16. The robot can climb up and down walls reliably with an average climbing speed of 200mm/s, a sideways moving speed of 100mm/s, and has a cleaning efficiency of 150m²/hour. These tests have proven the feasibility of the mechanical design and control system of the robot.

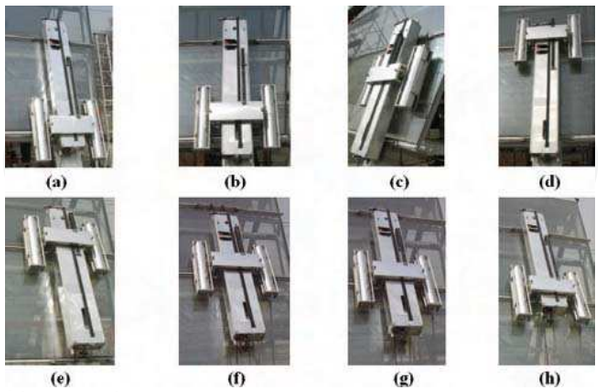

Fig. 24. Real climbing experiment.

2. An intelligent control system based on CAN bus was designed to control the robot. The advantages and the characteristics were analyzed. Some key issues such as sensor technology, which is necessary for such an autonomous robot, were studied in detail.
3. A kinematics model of climbing was concluded. The climbing dynamics of the robot are stated by the application of the Lagrange equation. All of the results are important for system design and the design of the controlling mechanism for this climbing robot.
4. The cleaning trajectory was determined and evaluated by the synthesis of work safety, cleaning efficiency and cleaning coverage percentage. Testing results with the robot have verified the effectiveness of the CCPP.

8. References

Sattar, T. P., Bridge, B., Chen, S., Zhao, Z. (2003). Development of CLAWER System that Combines the Tasks of Monitoring, Mobility, Manipulation, and Measurement for Industrial Inspection Tasks, Proceedings of CLAWAR 2003, Catania, Italy, September, 2003, pp.699-706.

Zhang, H.; Zhang, J.; Wang, W.; Zong, G. (2004). Design of a Pneumatic Glass Wall Cleaning Robot for High-Rise Buildings, Proceedings of the ASER '04 2nd International Workshop on Advances in Service Robotics, May 21, Stuttgart, Germany, pp.21-26.

Briones, L.; Brstamante, P.; Serna, M. A. (1994). Robicen: A wall-climbing pneumatic robot for inspection in nuclear power plants, Robotics & Computer-Integrated Manufacturing, Vol.11, No.4, pp. 287-292.

Luk, B. L.; White, T. S.; Cooke, D. S.; Hewer, N.D.; Hewer, G.; Chen, S. (2001). Climbing Service for Duct Inspection and Maintenance Applications in a Nuclear Reactor, Proceedings of the 32nd International Symposium on Robotics, 19-21 April, pp.41-45.

Liu, S.; Sheng, W.; Xu, D.; Wang, Y. (2000). Design of a New Wall Cleaning Robot with A Small Control System, High Technology Letters, Vol.10, No.9, pp.89-91.

Zhang, H.; Zhang, J.; Zong, G. (2004). Realization of a Service Climbing Robot for Glass-wall Cleaning, Proceedings of the 2004 International Conference on Intelligent

Mechatronics and Automation, August 26-31, Chengdu, China, pp.101-106.
Zhang, H., Zhang, J., Liu, R., Wang, W., Zong, G. (2004). Pneumatic Climbing Robots for Glass Wall Cleaning , Proceeding of the 7th International Conference on Climbing and Walking Robots and their Supporting Technologies for Mobile Machines, CLAWAR 2004, September 22-24, Madrid, Spain, pp. 1061-1070.
Zhang, H., Zhang, J., Wang, W., Liu, R., Zong, G. (2006). Sky Cleaner 3-A Real Pneumatic Climbing Robot for Glass-Wall Cleaning, IEEE Robotic & Automation Magazine, Vol.13, No.1 pp. 32-41.
Elkmann, N.; Felsch, T.; Sack, M.; Saenz, J.; Hortig, J. (2002). Innovative Service Robot Systems for Facade Cleaning of Difficult-to-Access Areas, Proceedings of the 2002 IEEE/RSJ International Conference on Intelligent Robots and Systems, EPFL, October 2002, Lausanne, Switzerland, pp.756-762.
Zhang, H. Research on The Wall Cleaning Robotic System for The High Buildings, Ph.D. Dissertation of Beijing University of Aeronautics and Astronautics, 2003.
Liu, R.; Zong, G.; Zhang, H.; Li, X. (2003). A Cleaning Robot for Construction Out-wall with Complicated Curve Surface, Proceedings of the Sixth International Conference on Climbing and Walking Robots and their Supporting Technologies for Mobile Machines, CLAWAR 2003, September, 2003, Catania, Italy, pp.825-834.
Zhang, H., Zhang, J., Liu, R., Zong, G. (2005.) Realization of a service robot for cleaning spherical surfaces, International Journal of Advanced Robotic Systems, Vol.2, No.1, pp. 53-58.
Fu, K.S., Gonzalez, R., Lee, C. (1987). Robotics: Control, sensing, Vision, and Intelligence, New York: McGraw-Hill.
Zhang, H.; Zhang, J.; Liu, R., Zong, G. (2005). Climbing Technique of the Cleaning Robot for a Spherical Surface, Proceedings of the 2005 International Conference on Intelligent Mechatronics and Automation, Ontario, Canada, July 29 - August 1, pp. 2061-2066.
Zelinsky, A., Jarvis, R.A., Byarne, J.C., Yuta, S. (1993). Panning Paths of Complete Coverage of an Unstructured Environment by a Mobile Robot, Proceedings of the ICAR93, pp. 533-538.
Neumann de Carvalho, R., Vidal, H. A., Vieira, P., Riberio, M. I. (1997). Complete Coverage Path Planning and Guidance for Cleaning Robots, Proceedings of ISIE'97, Guimaraes, Portugal, pp. 677-682.
Yang, S. X., Luo, C. (2004). A Neural Network Approach to Complete Coverage Path Planning, IEEE Transactions on System, Man, and Cybernetics-Part B: Cybernetics, Vol.34, No.1, pp.718-725.
Hofner, C., Schmidt, G. (1995). Path planning and Guidance Techniques for an Autonomous Mobile Robot, Robotics and Autonomous System, Vol.14, No. 2, pp. 199-212.
Pirzadeh, A., Snyder, W. (1990). A Unified Solution to Coverage and Search in Explored and Unexplored Terrains Using Indirect Control, Proceedings of IEEE Int. Conf. Robotics Automation, Raleigh, NC, pp.2113-2119.
Zhang, H.; Zhang, J.; Liu, R., Zong, G. (2005). Design of a Climbing Robot for Cleaning Spherical Surfaces, Proceeding of 2005 IEEE International Conference on Robotics and Biomimetics, Hong Kong, China, June 29-July 3, pp.375-380.
Zhang, H., Zhang, J., Liu, R., Zong, G. (2005). Effective Pneumatic Scheme and Control Strategy of a Climbing Robot for Class Wall Cleaning on High-rise Buildings, International Journal of Advanced Robotic Systems, Vol.3, No.2, 2006.

Mobile Robots: towards New Applications

Edited by Aleksandar Lazinica

ISBN 978-3-86611-314-5

Hard cover, 600 pages

Publisher I-Tech Education and Publishing

Published online 01, December, 2006

Published in print edition December, 2006

The range of potential applications for mobile robots is enormous. It includes agricultural robotics applications, routine material transport in factories, warehouses, office buildings and hospitals, indoor and outdoor security patrols, inventory verification, hazardous material handling, hazardous site cleanup, underwater applications, and numerous military applications. This book is the result of inspirations and contributions from many researchers worldwide. It presents a collection of wide range research results of robotics scientific community. Various aspects of current research in new robotics research areas and disciplines are explored and discussed. It is divided in three main parts covering different research areas: Humanoid Robots, Human-Robot Interaction, and Special Applications. We hope that you will find a lot of useful information in this book, which will help you in performing your research or fire your interests to start performing research in some of the cutting edge research fields mentioned in the book.

InTech Europe

University Campus STeP Ri
Slavka Krautzeka 83/A
51000 Rijeka, Croatia
Phone: +385 (51) 770 447
Fax: +385 (51) 686 166
www.intechopen.com

InTech China

Unit 405, Office Block, Hotel Equatorial Shanghai
No.65, Yan An Road (West), Shanghai, 200040, China
中国上海市延安西路65号上海国际贵都大饭店办公楼405单元
Phone: +86-21-62489820
Fax: +86-21-62489821

IntechOpen